

Seebeck coefficient of two-dimensional Dirac electrons in an organic conductor under pressure

Yoshikazu Suzumura¹ and Masao Ogata²

¹*Department of Physics, Nagoya University, Nagoya 464-8602, Japan*

²*Department of Physics and Trans-scale Quantum Science Institute, University of Tokyo, Bunkyo, Tokyo 113-0033, Japan**

(Dated: Received 29 October 2022; revised 22 April 2023; accepted 25 April 2023; published 9 May 2023)

The Seebeck coefficient, which is proportional to a ratio of the thermoelectric conductivity to electrical conductivity has been examined for Dirac electrons in the organic conductor α -(BEDT-TTF)₂I₃ [BEDT-TTF denotes a molecule given by bis(ethylenedithio)tetrathiafulvalene] under a uniaxial pressure using a two-dimensional tight-binding model with both impurity and electron-phonon (e-p) scatterings. We calculate an anomalous temperature (T) dependence of the Seebeck coefficient S_ν with $\nu = x$ (perpendicular to the molecular stacking axis) and y , which shows $S_\nu > 0$ with a maximum at high temperatures and $S_\nu < 0$ with a minimum at low temperatures. The microscopic mechanism of such a sign change of S_ν is clarified in terms of the spectral conductivity. The result is compared with experiments on α -(BEDT-TTF)₂I₃.

I. INTRODUCTION

The two-dimensional massless Dirac fermions,¹ which show a linear spectrum around the Dirac point have been studied extensively. Several properties as a bulk material are explored in an organic conductor² given by α -(BEDT-TTF)₂I₃, where BEDT-TTF denotes bis(ethylenedithio)tetrathiafulvalene.³ The conductor exhibits a zero-gap state (ZGS)⁴ and the transport property is characterized by the density of states (DOS), which vanishes linearly at the Fermi energy.⁵ The explicit band structure of the Dirac cone is obtained using a tight-binding (TB) model, where transfer energies under pressures are estimated from the extended Hückel method.^{6,7} The Dirac cone was verified by the first-principles density functional theory (DFT) calculation.⁸ Further a two-band model^{9,10} has been proposed to examine Dirac electrons in an organic conductor.

Characteristic properties of the Dirac cone appear in the temperature (T) dependence of physical quantities. Magnetic susceptibility with a T linear behavior at low temperatures shows a good correspondence between the theory and experiment.^{11–13} The chemical potential μ , which also depends on T , takes a significant role in the transport. The reversal of the sign of the Hall coefficient occurs when μ becomes equal to the energy of the Dirac point. Such a sign reversal of the Hall coefficient was proposed theoretically by assuming the extremely small amount of electron doping.¹⁴ The sign reversal was also observed experimentally in the Hall conductivity of α -(BEDT-TTF)₂I₃.¹⁵

Since the conductivity of Dirac electrons is fundamental as the transport, a two-band model with the conduction and valence bands has been studied, where the static conductivity at absolute zero temperature remains finite with a universal value, i.e., independent of the magnitude of impurity scattering owing to a quantum effect.¹⁶ At absolute zero temperature, the tilting of the Dirac cone provides the anisotropic conductivity and the de-

viation of the current from the applied electric field.¹⁷ At finite temperatures, the conductivity depends on the magnitude of the impurity scattering, Γ , which is proportional to the inverse of the life-time by the disorder. With increasing temperature, the conductivity increases for $\Gamma \ll T$.¹⁸ Although a monotonic increase in the conductivity is expected for such a model, the measured conductivity (or resistivity) on the above organic conductor shows an almost constant behavior at high temperatures.^{19–23} This is a noticeable transport of the Dirac electron in the presence of the electron-phonon (e-p) interaction, since the resistivity of the conventional metal at high temperatures increases linearly with respect to T due to the e-p scattering. The resistivity showing a nearly constant behavior at high temperatures is explained by the acoustic phonon scatterings using a simple two-band model of the Dirac cone without tilting.²⁴ Although the effect of the e-p scattering at high temperatures is qualitatively understood, the model should be improved to explain the conductivity of the actual organic conductor, where the energy band shows deviation from the linear spectrum.²⁵ Thus, the TB model with transfer energies of α -(BEDT-TTF)₂I₃ is examined to show that the presence of acoustic phonons gives rise to conductivity being nearly constant at high temperatures.²⁶

In addition to the electric conductivity, it is of interest to examine the thermoelectric (i.e., Seebeck) effect on the above model, where the T dependence of μ takes a crucial role. The Seebeck coefficient can be obtained microscopically in terms of linear response theory.^{27,28} However, we have to be careful in treating the heat current, because there are several forms of the heat current depending on the Hamiltonian.²⁹ In the case with impurity potentials and electron-phonon interactions, Jonson and Mahan³⁰ showed that the heat current \mathbf{J}_Q can be expressed as

$$\mathbf{J}_Q = \mathbf{J}_Q^{\text{kin}} + \mathbf{J}_Q^{\text{pot}} + \mathbf{J}_Q^{\text{e-p(I)}} + \mathbf{J}_Q^{\text{e-p(II)}} + \mathbf{J}_Q^{\text{ph}}, \quad (1)$$

(see, also Ref.²⁹), where $\mathbf{J}_Q^{\text{kin}}$, $\mathbf{J}_Q^{\text{pot}}$, and \mathbf{J}_Q^{ph} represent

the heat current operators originating from the kinetic energy of electrons, from the (impurity) potentials, and from the phonon Hamiltonian, respectively. The heat current due to the electron-phonon interaction, \mathbf{J}_Q^{e-p} , is divided into two contributions. If one takes account of only $\mathbf{J}_Q^{\text{kin}} + \mathbf{J}_Q^{\text{pot}} + \mathbf{J}_Q^{e-p(I)}$ as the heat current operator, one can show that Eqs. (14) and (15) below (called the Sommerfeld-Bethe relation) hold.²⁹ However, $\mathbf{J}_Q^{e-p(II)}$ and \mathbf{J}_Q^{ph} do not satisfy the Sommerfeld-Bethe relation and will give additional contributions in the electrothermal conductivity.^{29,30} For example, \mathbf{J}_Q^{ph} leads to the phonon drag effect.^{29,31,32} Jonson and Mahan also discussed that the contribution from $\mathbf{J}_Q^{e-p(II)}$ is small in nearly free electron systems. Thus, we do not consider this term and, in the following, we use the Sommerfeld-Bethe relation leaving the phonon-drag problem as a future problem.

So far, there are several theoretical studies on the Seebeck (and Nernst) effect in the Dirac electron systems,³³⁻³⁷ where the Seebeck coefficient exhibits the variety of the sign. In this paper, we study the Seebeck coefficient for the ZGS of Dirac electrons in the two-dimensional organic conductor, α -(BEDT-TTF)₂I₃. There have been several experimental and theoretical studies on this material. As for the experiments, the ZGS has been obtained under both uniaxial pressures above $P_a = 5$ kbar and hydrostatic pressures above 1.5 GPa.² Under the uniaxial pressures, the ZGS was found only for P_a corresponding to the pressure along the a direction.²¹ There are several measurements of resistivity suggesting the ZGS under the hydrostatic pressures.^{19,20,23} Regarding the Seebeck coefficient, the measurement has been performed only for hydrostatic pressures,^{38,39} where the sign change of the Seebeck coefficient with decreasing temperature occurs along the b direction.³⁸ However, another experiment³⁹ exhibits the positive Seebeck coefficient without the sign change. It could be ascribed to the effect of the hole doping, since the latter material is a different sample from the former one.

As for the theory, there is a work discussing the sign reversal for the Seebeck coefficient of α -(BEDT-TTF)₂I₃ under the hydrostatic pressure.³⁵ However, the sign of the Seebeck coefficient for the b direction obtained in this theory disagrees with that of the experiment.³⁸ This issue remains as a future problem. In the present paper, we examine the Seebeck coefficient for uniaxial pressures, although the experiment has not yet been performed. We will show the sign change of the Seebeck coefficient in this case.

The present paper is organized as follows. First, the model and formulation to calculate the Seebeck coefficient for α -(BEDT-TTF)₂I₃ with 3/4-filled band are given. Next, after calculating the T dependence of the chemical potential, we show the Seebeck coefficient with the electric conductivity, which is analyzed in terms of the spectral conductivity. Finally, discussions, summary, and comparison with the experiment are given.

II. FORMULATION

We consider a two-dimensional Dirac electron system per spin, which is given by

$$H = H_0 + H_p + H_{e-p} + H_{\text{imp}}. \quad (2)$$

H_0 describes a TB model of the organic conductor, α -(BEDT-TTF)₂I₃. H_p and H_{e-p} describe an acoustic phonon and an electron-phonon (e-p) interaction, respectively. H_{imp} is the impurity potential. The unit of the energy is taken as eV. Figure 1(a) shows the TB model for H_0 consisting of four BEDT-TTF molecules in the unit cell. H_0 is expressed as

$$\begin{aligned} H_0 &= \sum_{i,j=1}^N \sum_{\alpha,\beta=1}^4 t_{i,j;\alpha,\beta} a_{i,\alpha}^\dagger a_{j,\beta} \\ &= \sum_{\mathbf{k}} \sum_{\alpha,\beta=1}^4 h_{\alpha\beta}(\mathbf{k}) a_\alpha^\dagger(\mathbf{k}) a_\beta(\mathbf{k}), \end{aligned} \quad (3)$$

where $a_{i,\alpha}^\dagger$ denotes a creation operator of an electron of molecule α [= A(1), A'(2), B(3), and C(4)] in the unit cell at the i -th lattice site. N is the total number of square lattice sites and $t_{i,j;\alpha,\beta}$ denote the seven kinds of transfer energies $a_1, \dots, a_3, b_1, \dots, b_4$ between the nearest-neighbor (NN) sites as shown in Fig. 1(a). A Fourier transform for the operator $a_{j,\alpha}$ is given by $a_{j,\alpha} = 1/N^{1/2} \sum_{\mathbf{k}} a_\alpha(\mathbf{k}) \exp[i\mathbf{k} \cdot \mathbf{r}_j]$, where $\mathbf{k} = (k_x, k_y)$ and the lattice constant is taken as unity. H_0 is diagonalized by

$$\sum_{\beta} h_{\alpha\beta}(\mathbf{k}) d_{\beta\gamma}(\mathbf{k}) = E_\gamma(\mathbf{k}) d_{\alpha\gamma}(\mathbf{k}), \quad (4)$$

where $E_1(\mathbf{k}) > E_2(\mathbf{k}) > E_3(\mathbf{k}) > E_4(\mathbf{k})$.

The Dirac point (\mathbf{k}_D) is calculated from

$$E_1(\mathbf{k}_D) = E_2(\mathbf{k}_D) = \epsilon_D. \quad (5)$$

The ZGS is obtained when ϵ_D becomes equal to the chemical potential at $T = 0$. The chemical potential μ is determined from the three-quarter-filled condition, which is given by

$$\frac{1}{N} \sum_{\mathbf{k}} \sum_{\gamma} f(E_\gamma(\mathbf{k})) = 3, \quad (6)$$

where $f(\epsilon) = 1/(\exp[(\epsilon - \mu)/k_B T] + 1)$ with T being temperature and a Boltzmann constant taken as $k_B = 1$. Using the band energy $E_\gamma(\mathbf{k})$, the T dependence of μ is examined in the next paragraph.

On the basis of four molecules in the unit cell of Fig. 1(a), the matrix element of $h_{\alpha\beta}$ in Eq. (3) is expressed as $h_{12}(\mathbf{k}) = a_3 + a_2 Y$, $h_{13}(\mathbf{k}) = b_3 + b_2 X$, $h_{14}(\mathbf{k}) = b_4 Y + b_1 X Y$, $h_{23}(\mathbf{k}) = b_2 + b_3 X$, $h_{24}(\mathbf{k}) = b_1 + b_4 X$, $h_{34}(\mathbf{k}) = 2a_1$, $h_{11} = h_{22} = h_{33} = h_{44} = 0$ and $h_{\alpha\beta}(\mathbf{k}) = h_{\beta\alpha}^*(\mathbf{k})$, where $X = \exp[ik_x] = X^*$, and $Y = \exp[ik_y] = Y^*$. Although this model is complicated,

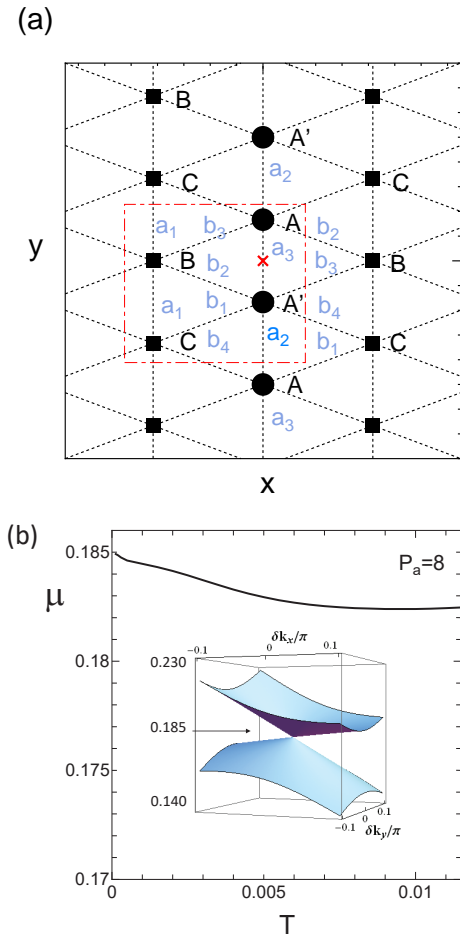


Figure 1. (a) Crystal structure, where there are four BEDT-TTF molecules A, A', B and C in the unit cell indicated by red lines, which forms a square lattice. Note that x (y) corresponds to the b (a) direction, which are perpendicular (parallel) to the molecular stacking axis. Seven transfer energies are shown by $a_1, \dots, a_3, b_1 \dots b_4$ for the nearest neighbor (NN) sites. The cross denotes an inversion center between two equivalent molecules A and A'. (b) Temperature (T) dependence of chemical potential (μ) at a uniaxial pressure $P_a = 8$ kbar. The unit is taken as eV. The inset denotes a pair of Dirac cones around a Dirac point, $\mathbf{k}_D = (0.55, 0.25)\pi$, where $(\delta k_x, \delta k_y) = \mathbf{k} - \mathbf{k}_D$ with the lattice constant taken as unity. The conduction and valence bands [$E_1(\mathbf{k})$ and $E_2(\mathbf{k})$] touch at \mathbf{k}_D with a band energy $\mu_0 = 0.185$ corresponding to the chemical potential at $T=0$.

when we use these transfer energies, we find the zero-gap state (ZGS) composed of Dirac electrons as shown in the inset of Fig. 1(b), which consistently explains several experimental results. For the uniaxial pressure P_a (kbar), which is applied to the a direction, transfer energies with NN sites, $t = a_1, \dots, b_4$ (eV), are estimated by the extended Hückel method based on the crystal structure analyses with the x ray diffraction measurement. Using the overlap integrals estimated from the coordinates of the BEDT-TTF molecules, transfer energies are obtained by multiplying -10 eV corresponding to the

atomic energy.^{3,6} From an interpolation method between $P_a = 0$ and 2 kbar,^{4,6} the transfer energies are given by $t(P_a) = t(0)(1 + K_t P_a)$, where $t(0) = a_1(0), \dots, b_4(0) = -0.028, -0.048, 0.020, 0.123, 0.140, 0.062$, and 0.025 , and $K_t = 0.089, 0.167, -0.025, 0, 0.011$, and 0.032 , respectively. Note that the ZGS is obtained for $P_a > 3$ kbar.

In Fig. 1(b), the chemical potential μ is shown as a function of T with a fixed $P_a = 8$ kbar, which decreases with increasing for $T (< 0.01)$. At $T = 0$, the chemical potential is given by $\mu_0 = 0.185$, resulting in the ZGS as shown on the plane of $\delta \mathbf{k} = \mathbf{k} - \mathbf{k}_D$ (the inset), where the conduction and valence bands touch at a Dirac point $\mathbf{k}_D = (0.55, 0.25)\pi$. The Dirac cone is tilted almost along the k_x axis, which gives rise to an anisotropy of the transport property. With increasing T , μ decreases and takes a slight minimum $\mu = 0.1824$ at $T \simeq 0.01$. The decrease of μ suggests that the hole exists in the valence band below the Dirac point. The choice of $P_a = 8$ kbar is large as the extrapolation, but could be used considering the following facts. The Dirac point with increasing P_a is robust due to a small variation of \mathbf{k}_D compared with the distance from the Γ point ($\mathbf{k} = 0$), where a pair of Dirac points merges at $P_a \simeq 40$ kbar.² Furthermore, the ZGS has been observed up to $P_a = 10$ kbar in the experiment of the resistivity.²¹

In Eq. (2), the second term denotes the harmonic phonon given by $H_p = \sum_{\mathbf{q}} \omega_{\mathbf{q}} b_{\mathbf{q}}^\dagger b_{\mathbf{q}}$ with $\omega_{\mathbf{q}} = v_s |\mathbf{q}|$ and $\hbar = 1$. The third term is the e-p interaction with a coupling constant $g_{\mathbf{q}}$, where⁴⁰.

$$H_{e-p} = \sum_{\mathbf{k}, \gamma} \sum_{\mathbf{q}} g_{\mathbf{q}} c_{\gamma}(\mathbf{k} + \mathbf{q})^\dagger c_{\gamma}(\mathbf{k}) (b_{\mathbf{q}} + b_{-\mathbf{q}}^\dagger), \quad (7)$$

with $c_{\gamma}(\mathbf{k}) = \sum_{\alpha} d_{\alpha\gamma} a_{\alpha}(\mathbf{k})$. The e-p scattering is considered within the same band (i.e., intraband) owing to the energy conservation with $v \gg v_s$, where $v \simeq 0.05$ ¹¹ denotes the averaged velocity of the Dirac cone. The last term of Eq. (2), H_{imp} , denotes a normal impurity scattering.

The spectral conductivity $\sigma_{\nu}(\epsilon, T)$ with $\nu = x$ and y is calculated as

$$\begin{aligned} \sigma_{\nu}(\epsilon, T) &= \frac{e^2}{\pi \hbar N} \sum_{\mathbf{k}} \sum_{\gamma, \gamma'} v_{\gamma\gamma'}^{\nu}(\mathbf{k})^* v_{\gamma'\gamma}^{\nu}(\mathbf{k}) \\ &\times \frac{\Gamma_{\gamma}}{(\epsilon - E_{\gamma}(\mathbf{k}))^2 + \Gamma_{\gamma}^2} \times \frac{\Gamma_{\gamma'}}{(\epsilon - E_{\gamma'}(\mathbf{k}))^2 + \Gamma_{\gamma'}^2}, \end{aligned} \quad (8)$$

$$v_{\gamma\gamma'}^{\nu}(\mathbf{k}) = \sum_{\alpha\beta} d_{\alpha\gamma}(\mathbf{k})^* \frac{\partial h_{\alpha\beta}}{\partial k_{\nu}} d_{\beta\gamma'}(\mathbf{k}), \quad (9)$$

where $h = 2\pi\hbar$ denotes Planck's constant. The spectral conductivity depends on T due to the e-p interaction. In fact, Γ_{γ} denotes the damping of the electron of the γ band given by

$$\Gamma_{\gamma} = \Gamma + \Gamma_{\text{ph}}^{\gamma}, \quad (10)$$

where the first term comes from the impurity scattering and the second term corresponding to the phonon scattering is given by^{24,26,41}

$$\Gamma_{\text{ph}}^\gamma = C_0 R \times T |\xi_{\gamma, \mathbf{k}}|, \quad (11a)$$

$$R = \frac{\lambda}{\lambda_0}, \quad (11b)$$

where $\lambda = |g_{\mathbf{q}}|^2/\omega_{\mathbf{q}}$, $\xi_{\gamma, \mathbf{k}} = E_\gamma(\mathbf{k}) - \mu$, $C_0 = 6.25\lambda_0/(2\pi v^2)$ and $\lambda_0/2\pi v = 0.1$. λ_0 corresponds to λ for an organic conductor^{42,43} and λ becomes independent of $|\mathbf{q}|$ for small $|\mathbf{q}|$. R is taken as a parameter. We take $\Gamma = 0.0005$ and $R=0.5$ as in the previous paper,²⁴ where a choice of $R=0.5$ gives a reasonable suppression of the conductivity at high T , and $\Gamma = 0.0005$ corresponds to a weak impurity scattering due to Γ being much smaller than T .

In linear response theory, the electric current density $\mathbf{j} = (j_x, j_y)$ is obtained by the electric field $\mathbf{E} = (E_x, E_y)$ and the temperature gradient ∇T , i.e., the ν ($= x$ and y) component of the current density, is expressed as

$$j_\nu = L'_{11} E_\nu - L'_{12} \nabla_\nu T / T, \quad (12)$$

where L'_{11} is the electrical conductivity σ_ν ²⁵ and L'_{12} is the thermoelectric conductivity.

From (12), the Seebeck coefficient S_ν is obtained by

$$S_\nu(T) = \frac{L'_{12}}{T L'_{11}}. \quad (13)$$

As discussed in the introductory part, in terms of Eq. (8), we calculate L'_{11} and L'_{12} from the Sommerfeld-Bethe relation,

$$L'_{11} = \sigma_\nu(T) = \int_{-\infty}^{\infty} d\epsilon \left(-\frac{\partial f(\epsilon)}{\partial \epsilon} \right) \times \sigma_\nu(\epsilon, T), \quad (14)$$

$$L'_{12} = \frac{-1}{e} \int_{-\infty}^{\infty} d\epsilon \left(-\frac{\partial f(\epsilon)}{\partial \epsilon} \right) \times (\epsilon - \mu) \sigma_\nu(\epsilon, T), \quad (15)$$

where $e(> 0)$ denotes the electric charge. Noting that $-\partial f(\epsilon)/\partial \epsilon$ is the even function of $\epsilon - \mu$, and $\sigma_\nu(\epsilon, T)$ in Eq. (14) can be expanded as

$$\begin{aligned} \sigma_\nu(\epsilon, T) &= \sigma_\nu(\mu, T) + \sigma'_\nu(\mu, T)(\epsilon - \mu) \\ &\quad + \frac{1}{2} \sigma''_\nu(\mu, T)(\epsilon - \mu)^2 + \dots, \end{aligned} \quad (16)$$

Eq. (15) is calculated as

$$\begin{aligned} eL'_{12}(T) &= -\frac{\pi^2}{3} \sigma'_\nu(\mu, T) T^2 - \frac{7\pi^4}{90} \sigma'''_\nu(\mu, T) T^4 \\ &\quad + \dots, \end{aligned} \quad (17)$$

at low temperatures. It is shown later that the sign change of $S_\nu(T)$ with decreasing T comes from that of the first term of Eq. (17).

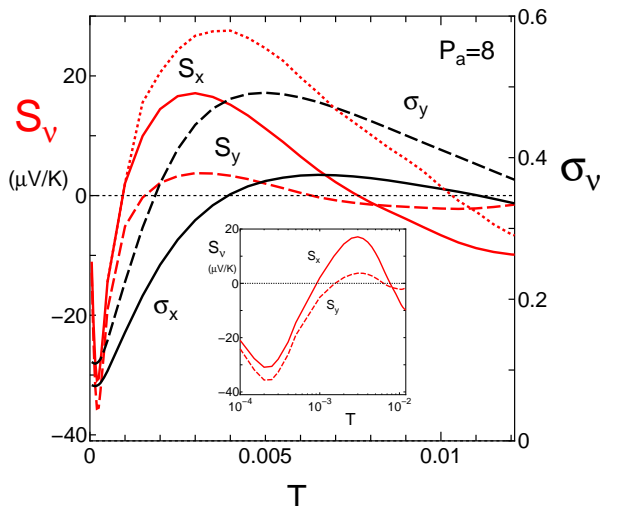


Figure 2. T dependence of the Seebeck coefficients S_x (red solid line) and S_y (red dashed line) for $P_a = 8$ kbar, which are compared with electric conductivities σ_x (solid line) and σ_y (dashed line). The e-p coupling is taken as $R=0.5$. The dotted line shows S_x for $R=0$. The inset denotes the magnified S_x and S_y , which suggest $S_\nu \rightarrow 0$ at $T \rightarrow 0$.

III. SEEBECK COEFFICIENT

Now we study $S_\nu(T)$ using parameters of α -(BEDT-TTF)₂I₃. The Seebeck coefficient of α -(BEDT-TTF)₂I₃ under uniaxial pressures provides the following T dependence. In the present paper, we take $P_a = 8$, which shows a sign change, where $S_x(T) > 0 (< 0)$ at high temperatures (at low temperatures). Figure 2 shows the T dependence of the Seebeck coefficient, S_ν and the electrical conductivity σ_ν , where $\sigma_y > \sigma_x$ for any T and $S_x > S_y$ for $T < 0.008$. Note that both S_x and S_y exhibit the change of the sign at low temperatures. It is found that $S_x = 0$ at $T \simeq 0.0009$ and that S_x takes a maximum $\simeq 17 \mu\text{V}/\text{K}$ at $T \simeq 0.003$. At low temperatures given by $S_x < 0$, S_x takes a minimum. Similar behavior is also obtained for S_y , where $S_y = 0$ at $T \simeq 0.0015$ and the temperatures corresponding to the maximum and minimum are almost the same as those of S_x . The relation $\sigma_y > \sigma_x$, which comes from the tilted Dirac cone [Fig. 1(b)],¹⁷ results in $S_x > S_y > 0$. The inset denotes magnified S_ν at low temperatures. A minimum exists at $T \simeq 0.0002$ and the extrapolation to lower temperatures suggests $S_\nu \propto -T$ since $S_\nu \sim -T \sigma'_\nu(\mu, T) / \sigma_\nu(\mu, T)$ [see Eqs. (16) and (17)]. The interband effect ($\gamma \neq \gamma'$) becomes small at low temperatures and the increase of Γ gives a slight reduction of S_ν . The decrease of the uniaxial pressure P reduces the temperature region for $S_x > 0$. Note that there is enough range of P_a for a sign change of S_x , which is in general sensitive to parameters. In fact, S_x for $P_a = 6$ kbar (not shown here) also shows the sign change at $T \simeq 0.0005$.

In order to comprehend the existence of $S_x(T) = 0$,

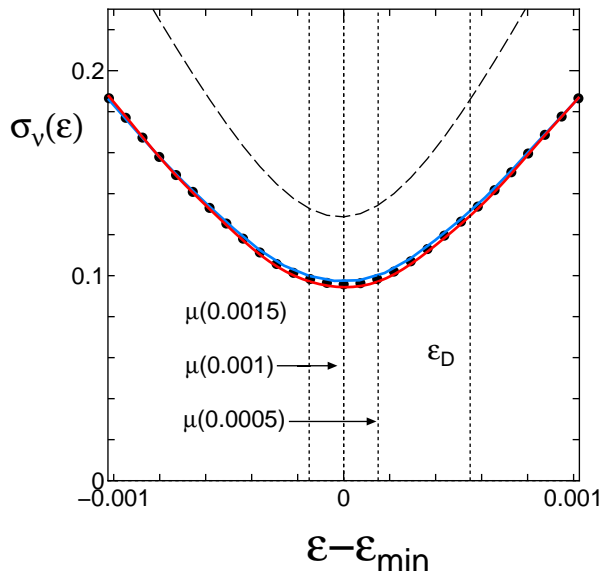


Figure 3. Spectral conductivity $\sigma_\nu(\epsilon, T)$ for $\nu = x$ as a function of $\epsilon - \epsilon_{\min}$, which are obtained for $T = 0.0005$ (red line), 0.001 (dots), and 0.0015 (blue line). $\epsilon_{\min} \simeq \mu(0.001)$. The dashed line shows σ_y for $T = 0.001$. The vertical lines denote locations of the chemical potential $\mu(T)$ for $\epsilon_D = \mu(0) \simeq 0.1850$, $\mu(0.0005) \simeq 0.1846$, $\mu(0.001) \simeq 0.1845$, and $\mu(0.0015) \simeq 0.1843$ [(Fig. 1(b))]. The case of $\mu(T) < \epsilon_{\min}$ gives $S_\nu > 0$, while the case of $\mu(T) > \epsilon_{\min}$ suggests $S_\nu < 0$.

we examine the spectral conductivity. In Fig. 3, spectral conductivity $\sigma_\nu(\epsilon, T)$ is shown as a function of $\epsilon - \epsilon_{\min}$, where $\sigma_\nu(\epsilon, T)$ takes a minimum at $\epsilon_{\min} = 0.18447$. The minimum is close but lower than that of the Dirac point ϵ_D ($\epsilon_D - \epsilon_{\min} \simeq 0.0005$). $S_x(T) = 0$ occurs when $\mu(T) \simeq \epsilon_{\min}$ at some temperature. A similar minimum is obtained for $\sigma_y(T)(\epsilon, 0.001)$ (dashed line), which is larger than $\sigma_x(\epsilon, 0.001)$. $\sigma_x(\epsilon, T)$ is shown for the fixed $T = 0.0005, 0.001$ and 0.0015 , where the width depends on T due to $\Gamma_{\text{ph}}^\gamma$ (Eq. 11a). The vertical lines denote the corresponding $\mu(T)$, where $\mu(0.001) = \epsilon_{\min}$ and $\epsilon_D = \mu(0)$. Since $\mu(0.0015) < \mu(0.001) < \mu(0.0005)$, $\sigma_x'(T) > 0$ for $T < 0.001$ and $\sigma_x'(T) < 0$ for $T > 0.001$. From Eq. (17), it turns out that $S_\nu > 0$ is obtained for $\mu(T) < \epsilon_{\min}$ and $S_\nu < 0$ is obtained for $T \simeq 0.00095 < 0.001$, i.e., for $\mu(T)$ being slightly lower than ϵ_{\min} due to the second term of Eq. (17). Thus, with decreasing T , $S_\nu(T)$ changes the sign from a positive to a negative one at $\mu \simeq \epsilon_{\min}$ corresponding to $\sigma'_\nu(\mu, T) = 0$. Note that the sign change of S_ν in Fig. 2 is obtained in the case of $\mu < \epsilon_D$. This fact is different from that of the Hall coefficient,¹⁴ where the sign change occurs at $\mu = \epsilon_D$.

Here we note the minimum and maximum of S_ν in Fig. 2. Such a behavior is also obtained only for the impurity scattering, i.e., without the e-p coupling ($R=0$). Compared with the dotted line in Fig. 2, S_x at high temperature is reduced by the e-p coupling, while S_x at low temperatures ($T < 0.001$) remains the same. We also examined S_ν at lower pressures. For $P_a=6$, it is found

that S_x decreases and S_y increases, while the maximum and minimum still exist. The spectral conductivity $\sigma_\nu(\epsilon)$ shows the existence of the minimum and the T dependence of the chemical potential similar to Fig. 3.

IV. DISCUSSIONS AND SUMMARY

Here, we discuss the relevance of our result to experiments. The temperatures of the sign change and the maximum of $S_x (> 0)$ in Fig. 2 are similar to those obtained in the experiment under the hydrostatic pressures.³⁸ Although this is suggestive, note that the experiment is carried out in the hydrostatic pressure, while our calculation is for the uniaxial pressure. As another aspect, a minimum of S_x at low temperature, suggesting $S_x \rightarrow 0$ at $T = 0$, is an interesting piece of information from our calculation, that should be examined experimentally by decreasing the temperature.

Finally, let us comment on the Seebeck coefficient in the case of the hydrostatic pressure. The previous theory³⁵ studied the effect of short-range repulsive interactions on the TB model with the transfer energies obtained from the first-principles calculation,⁸ and showed that the decrease of T leads to the sign change from $S_y > 0$ into $S_y < 0$ at $T \simeq 0.0002$. Noting that the Seebeck coefficients are in general sensitive to parameters such as transfer energies and site potentials, we examined S_x and S_y for the following two cases. One is a model used in the previous calculation^{11,26} (but slightly different from that used in Ref.³⁵), in which the transfer energies obtained from the first-principles calculation⁸ are fixed at a low temperature, and the site potentials obtained from the mean field of the interaction are taken as those at $T = 0$. In this case, we obtained $S_y > 0$ at high temperatures followed by the sign change at low temperatures, while S_x is negative at any temperature. The other is a model in which the transfer energies are obtained by crystal structure analyses at $P = 1.76$ GPa.⁷ Using a choice of site potentials that gives a ZGS,⁷ we obtained that $S_y > 0$ at high temperatures with the sign change at a temperature being slightly higher than that in the former model, while S_x is negative at any temperature. Thus, we found $S_x < 0$ as a common feature of the above two models, which is inconsistent with the experiment.³⁸ It remains a future problem to obtain a reliable TB model exhibiting the sign change of S_x for hydrostatic pressures.

In summary, for the T dependence of the Seebeck coefficient of α -(BEDT-TTF)₂I₃, $S_\nu(T)$ under uniaxial pressures was calculated although there is no experiment at present. We obtained the sign change for both S_x and S_y and clarified the microscopic mechanism in terms of the spectral conductivity $\sigma_\nu(\mu, T)$. The correspondence of the present theory to the experiment awaits the future measurement of the Seebeck coefficient under uniaxial pressures.

ACKNOWLEDGMENTS

We thank N. Tajima for useful discussions and for providing us with data of the Seebeck coefficient of α -

(BEDT-TTF)₂I₃ at 1.9 GPa. This work is supported by JST-Mirai Program Grant (Grant No. JPMJMI19A1).

-
- * ogata@phys.s.u-tokyo.ac.jp
- ¹ K. S. Novoselov, A. K. Geim, S. V. Morozov, D. Jiang, M. I. Katsnelson, I. V. Grigorieva, S. V. Dubonos, and A. A. Firsov, *Nature* **438**, 197 (2005).
 - ² K. Kajita, Y. Nishio, N. Tajima, Y. Suzumura, and A. Kobayashi, *J. Phys. Soc. Jpn.* **83**, 072002 (2014).
 - ³ T. Mori, A. Kobayashi, Y. Sasaki, H. Kobayashi, G. Saito, and H. Inokuchi, *Chem. Lett.* **13**, 957 (1984).
 - ⁴ S. Katayama, A. Kobayashi, and Y. Suzumura, *J. Phys. Soc. Jpn.* **75**, 054705 (2006).
 - ⁵ A. Kobayashi, S. Katayama, K. Noguchi, and Y. Suzumura, *J. Phys. Soc. Jpn.* **73**, 3135 (2004).
 - ⁶ R. Kondo, S. Kagoshima, and J. Harada, *Rev. Sci. Instrum.* **76**, 093902 (2005).
 - ⁷ R. Kondo, S. Kagoshima, N. Tajima, and R. Kato, *J. Phys. Soc. Jpn.* **78**, 114714 (2009).
 - ⁸ H. Kino and T. Miyazaki, *J. Phys. Soc. Jpn.* **75**, 034704 (2006).
 - ⁹ A. Kobayashi, S. Katayama, Y. Suzumura, and H. Fukuyama, *J. Phys. Soc. Jpn.* **76**, 034711 (2007).
 - ¹⁰ M. O. Goerbig, J.-N. Fuchs, G. Montambaux, and F. Piéchon, *Phys. Rev. B* **78**, 045415 (2008).
 - ¹¹ S. Katayama, A. Kobayashi, and Y. Suzumura, *Eur. Phys. J. B* **67**, 139 (2009).
 - ¹² Y. Takano, K. Hiraki, Y. Takada, H. M. Yamamoto, and T. Takahashi, *J. Phys. Soc. Jpn.* **79**, 104704 (2010).
 - ¹³ M. Hirata, K. Ishikawa, K. Miyagawa, M. Tamura, C. Berthier, D. Basko, A. Kobayashi, G. Matsuno, and K. Kanoda, *Nat. Commun.* **7**, 12666 (2016).
 - ¹⁴ A. Kobayashi, Y. Suzumura, and H. Fukuyama, *J. Phys. Soc. Jpn.* **77**, 064718 (2008).
 - ¹⁵ N. Tajima, R. Kato, S. Sugawara, Y. Nishio, and K. Kajita, *Phys. Rev. B* **85**, 033401 (2012).
 - ¹⁶ N. H. Shon and T. Ando, *J. Phys. Soc. Jpn.* **67**, 2421 (1998).
 - ¹⁷ Y. Suzumura, I. Proskurin, and M. Ogata *J. Phys. Soc. Jpn.* **83**, 023701 (2014).
 - ¹⁸ N. M. R. Peres, F. Guinea, and A. H. Castro Neto, *Phys. Rev. B* **83**, 125411 (2006).
 - ¹⁹ K. Kajita, T. Ojio, H. Fujii, Y. Nishio, H. Kobayashi, A. Kobayashi, and R. Kato, *J. Phys. Soc. Jpn.* **61**, 23 (1992).
 - ²⁰ N. Tajima, M. Tamura, Y. Nishio, K. Kajita, and Y. Iye, *J. Phys. Soc. Jpn.* **69**, 543 (2000).
 - ²¹ N. Tajima, A. Ebina-Tajima, M. Tamura, Y. Nishio, and K. Kajita, *J. Phys. Soc. Jpn.* **71**, 1832 (2002).
 - ²² N. Tajima, S. Sugawara, M. Tamura, R. Kato, Y. Nishio, and K. Kajita, *EPL* **80**, 47002 (2007).
 - ²³ D. Liu, K. Ishikawa, R. Takehara, K. Miyagawa, M. Tamura, and K. Kanoda, *Phys. Rev. Lett.* **116**, 226401 (2016).
 - ²⁴ Y. Suzumura and M. Ogata, *Phys. Rev. B* **98**, 161205 (2018).
 - ²⁵ S. Katayama, A. Kobayashi, and Y. Suzumura, *J. Phys. Soc. Jpn.* **75**, 023708 (2006).
 - ²⁶ Y. Suzumura, and M. Ogata, *J. Phys. Soc. Jpn.* **90**, 044709 (2021).
 - ²⁷ R. Kubo, *J. Phys. Soc. Jpn.* **12**, 570 (1957).
 - ²⁸ J. M. Luttinger, *Phys. Rev.* **135**, A1505 (1964).
 - ²⁹ M. Ogata, and H. Fukuyama, *J. Phys. Soc. Jpn.* **88**, 074703 (2019).
 - ³⁰ M. Jonson and G. D. Mahan, *Phys. Rev. B* **42**, 9350 (1990).
 - ³¹ H. Matsuura, M. Maebashi, M. Ogata, and H. Fukuyama, *J. Phys. Soc. Jpn.* **88**, 074601 (2019).
 - ³² H. Matsuura, M. Ogata, T. Mori, and E. Bauer, *Phys. Rev. B* **104**, 214421 (2021).
 - ³³ I. Proskurin, and M. Ogata, *J. Phys. Soc. Jpn.* **82**, 063712 (2013).
 - ³⁴ T. Yamamoto and H. Fukuyama, *J. Phys. Soc. Jpn.* **87**, 114710 (2018).
 - ³⁵ D. Ohki, Y. Omori, and A. Kobayashi, *Phys. Rev. B* **101**, 245201 (2020).
 - ³⁶ T. Mizoguchi, H. Matsuura, and M. Ogata, *Phys. Rev. B* **105**, 205203 (2022).
 - ³⁷ J. Fujimoto, and M. Ogata, *J. Phys. Soc. Jpn.* **91**, 054603 (2022).
 - ³⁸ R. Kitamura, N. Tajima, K. Kajita, R. Kato, M. Tamura, T. Naito, and Y. Nishio, *JPS Conf. Proc.* **1**, 012097 (2014); N. Tajima (private communication).
 - ³⁹ T. Konoike, M. Sato, K. Uchida, and T. Osada, *J. Phys. Soc. Jpn.* **82**, 073601 (2013).
 - ⁴⁰ H. Fröhlich, *Proc. R. Soc. Lond. A* **223**, 296 (1954).
 - ⁴¹ A. A. Abrikosov, L. P. Gorkov, and I. E. Dzyaloshinskii, *Methods of Quantum Field Theory in Statistical Physics* (Prentice-Hall, Englewood Cliffs, NJ, 1963).
 - ⁴² M. J. Rice, L. Pietronero, and P. Brüesch, *Solid State Commun.* **21**, 757 (1977).
 - ⁴³ H. Gutfreund, C. Hartzstein, and M. Weger *Solid State Commun.* **36**, 647 (1980).